FRONTIERS OF PHYSICS

RESEARCH ARTICLE
Volume 17 / Issue 5 / 51502 / 2022

Error-detected three-photon hyperparallel Toffoli gate with state-selective reflection

Yi-Ming Wu, Gang Fan, Fang-Fang Du†

Science and Technology on Electronic Test and Measurement Laboratory, North University of China, Taiyuan 030051, China
Corresponding author. E-mail: †duff@nuc.edu.cn
Received March 30, 2022; accepted May 11, 2022

ABSTRACT

We present an error-detected hyperparallel Toffoli (hyper-Toffoli) gate for a three-photon system based on the interface between polarized photon and cavity-nitrogen-vacancy (NV) center system. This hyper-Toffoli gate can be used to perform double Toffoli gate operations simultaneously on both the polarization and spatial-mode degrees of freedom (DoFs) of a three-photon system with a low decoherence, shorten operation time, and less quantum resources required, in compared with those on two independent three-photon systems in one DoF only. As the imperfect cavity-NV-center interactions are transformed into the detectable failures rather than infidelity based on the heralding mechanism of detectors, a near-unit fidelity of the quantum hyper-Toffoli gate can be implemented. By recycling the procedures, the efficiency of our protocol for the hyper-Toffoli gate is improved further. Meanwhile, the evaluation of gate performance with achieved experiment parameters shows that it is feasible with current experimental technology and provides a promising building block for quantum compute.

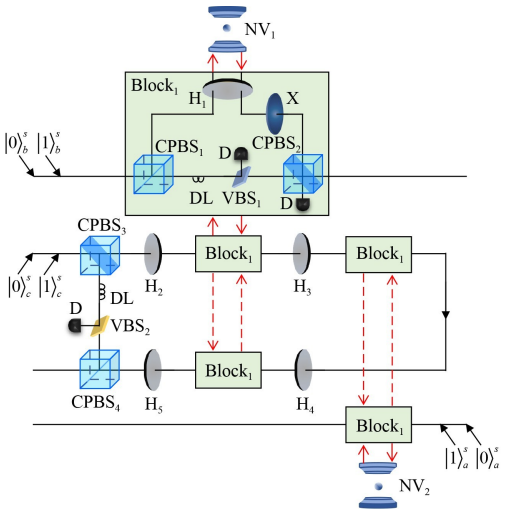

Keywords hyperparallel Toffoli gate, photon system, quantum information processing

1 Introduction

Compared to the best-known classical information processing, quantum information processing (QIP) [1], adhered to the principles of quantum mechanics, has great advantages in secure communication [2–7], algorithm [8–10], and machine learning [11–14], due to its great security and super-fast computing speed. Basic quantum logic gates are the building block of quantum computing, so they are regarded as an important unit of QIP. However, they still face the challenge of large-scale integration in practice. Therefore, to simplify the constantly growing complexity of qubits and decrease the overheads of resources, multi-qubit gates become the central ingredients in scalable QIP. Generally, the simplest universal multi-qubit gates is Toffoli or Fredkin gate [15, 16]. To construct an n-qubit Toffoli gate, $[(4^n - 3n - 1)/4]$ two-qubit gates by Shende *et al.* [17] can be required. Ralph *et al.* introduced qudit to model Toffoli gate with polynomial two-qubit gates [18], where the qudit takes advantage of ancillary higher-dimensional spaces. Based on multi-level physical systems, Radu *et al.* [19] presented the generalized n-qubit Toffoli gate using $n+1$ subsystems. Yu *et al.* [20] deemed five two-qubit gates as optimal for implementing the three-qubit Toffoli gate in theory. Fiurášek *et al.* [21] proposed a linear-optics-based quantum Toffoli gate. Soeken *et al.* [22] investigated the relationships between Pauli matrices and quantum

Higher Education Press

arXiv: 2206.07336
https://doi.org/10.1007/s11467-022-1172-3

logical gates for simplifying the quantum circuits. Recently, some physical architectures, including superconducting circuits [23–25], nitrogen-vacancy (NV) centers [26], quantum dots (QDs) [27–29], and trapped ions, [30] have been proposed to implement extensive Toffoli gates in experiment and theory.

Less resources required from quantum gates is crucial in quantum computation, originating from two strategies. One is to exploit a system with additional qudit [31–33], the other one is to encode the quantum information in multiple degrees of freedom (DoFs) of a system in universal computational tasks, i.e., hyperparallel quantum gates [34–40] simultaneously operating more than one independent operations. The hyper-parallel quantum computing can simplify the quantum circuit, improve the information-processing speed, reduce the quantum resource consumption, and suppress the photonic dissipation noise. Recently, implementing hyper-parallel photon-based controlled-NOT (CNOT) gate [34–37], hyper-parallel photon-matter-based universal CNOT gate [38], and hyper-parallel photon-based Toffoli gate [39] have been proposed. Ru *et al.* [40] have realized a deterministic quantum Toffoli gate on one photon in orbital-angular-momentum and polarization DoFs. Therefore, enquiry of the hyper-parallel multi-qubit Toffoli gate will be provided with great significance in scalable hyper-parallel QIP.

Up to now, solid-state-spin systems play a promising platform for the realization of quantum computing, as solid-state nature combined with nanofabrication techniques provide a useful way to incorporate the electronic spins into optical microcavities [41–44]. One appealing type of solid-state-spin system is the electron spin in a NV center [45–47], which not only provides convenient ways of optical initialization, single-qubit manipulation, and high-fidelity readout at room temperature, but also processes a milliseconds coherence time of the electron spin in NV center, resorting to spin echo techniques [48, 49]. In recent years, the NV centers have numerous applications, such as distributed quantum computing [50], the hybrid quantum gates acting on the electron spin and the nearby nuclear spin [51], geometric single-qubit gates [52], CNOT gate [36, 53], and universal gates on NV center electronic [37] or photonic qubits [54, 55]. Moreover, NV-center-emission-based entanglement [56] and hyperentanglement purification [57] were also proposed recently.

In this paper, we propose an error-detected hyper-parallel Toffoli gate for a three-photon system assisted by the state-selective reflection of one-sided cavity-NV-center system. Our scheme has some characters. First, this hyper-Toffoli gate is equivalent to perform double Toffoli gate operations simultaneously on both the polarization and spatial DoFs of a three-photon system with a low decoherence, short operation time, and less quantum resources required, in compared with those on two independent three-photon systems in one DoF only. Second, the fidelity of the quantum hyper-Toffoli gate is unity in principle, as the inevitable imperfect performances can be detected by single-photon detectors. Third, the strong coupling limitations can be avoided, reducing the experimental conditions. Fourth, the success of the error-detected scheme can be heralded by the single-photon detectors. Fifth, the efficiency of the scheme can be further improved by repeating the operation processes when the detectors are clicked.

2 Hyper-paralleled quantum Toffoli gate

The cavity-NV center system is originated from a diamond NV center that is coupled to an optical one-sided cavity, as shown in Fig. 1. The bottom mirror of the optical cavity is partially reflection and the top one is 100% reflection. The negatively charged NV center in the diamond lattice is composed by a substitutional nitrogen atom, an adjacent vacancy and six electrons. Here, the spin-ground state of the negatively charged NV center owing to spin-spin interaction is split into $|0\rangle(m_s = 0)$ and $|\pm 1\rangle(m_s = \pm 1)$ with a 2.87GHz zero-field splitting. $|A_2\rangle = (|E_-\rangle|+1\rangle + |E_+\rangle|-1\rangle)/\sqrt{2}$ is one of the six excited states of the negatively charged NV center [58], taking into account spin–orbit and spin–spin interactions at the same time, and is robust due to stable symmetric property. $|E_\pm\rangle|(J_s = \pm 1)$ is orbit states of the cavity-NV center system. The optical transition $|+1\rangle \leftrightarrow |A_2\rangle$ ($|-1\rangle \leftrightarrow |A_2\rangle$) is driven by the absorption or emission of a left-(right-) circularly polarized photon $|R\rangle$ ($|L\rangle$), which can be improved by the NV center trapped in a frequency-degenerate two-mode cavity. The above polarized states can be rewrote as $|R\rangle = |0\rangle^p$, $|L\rangle = |1\rangle^p$ in the following presentation. Under the rotating wave approximation, the Hamiltonian of the cavity-NV-center system can be written as [59]

$$H = \omega_d \hat{\sigma}_+ \hat{\sigma}_- + \omega_c \hat{a}^\dagger \hat{a} + ig(\hat{\sigma}_+ \hat{a} - \hat{a}^\dagger \hat{\sigma}_-), \quad (1)$$

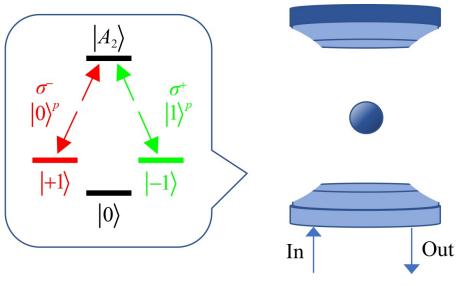

Fig. 1 A cavity-NV center system consists of the negatively charged NV center confined in an optical one-sided cavity. The optical transitions from the spin-ground states $|\pm 1\rangle$ to the excited state $|A_2\rangle$ are coupled by the $|\sigma_\mp\rangle$ circularly polarized photons.

where ω_d and ω_c denote the frequencies of the negatively charged NV center and the cavity field, respectively. $\hat{\sigma}_+$ and $\hat{\sigma}_-$ are the lifting and lowering operators of the negatively charged NV center. $\hat{a}$ and $\hat{a}^\dagger$ are the annihilation and creation operators of the cavity filed. g is the coupling strength between the NV center and the one-sided cavity.

The Heisenberg–Langevin equations about the operators $\hat{a}$ and $\hat{\sigma}_-$, and the input–output relationship of cavity field could be described as [60]

$$\begin{aligned}\frac{\mathrm{d}\hat{a}}{\mathrm{d}t} &= -\left[\mathrm{i}\left(\omega_c-\omega_p\right)+\frac{\kappa}{2}\right]\hat{a}-g\hat{\sigma}_- \\ &\quad -\sqrt{\kappa}\hat{a}_{in}+\hat{H}, \\ \frac{\mathrm{d}\hat{\sigma}_-}{\mathrm{d}t} &= -\left[\mathrm{i}\left(\omega_d-\omega_p\right)+\frac{\gamma}{2}\right]\hat{\sigma}_- -g\hat{\sigma}_z\hat{a} \\ &\quad +\sqrt{\gamma}\hat{\sigma}_z\hat{b}_{in}+\hat{G}, \\ \hat{a}_{out} &= \hat{a}_{in}+\sqrt{\kappa}\hat{a}. \end{aligned} \tag{2}$$

Here, ω_p represents the frequency of the input photon. $\hat{\sigma}_z=\hat{\sigma}_+\hat{\sigma}_- -\hat{\sigma}_-\hat{\sigma}_+$ is the population operator. κ and γ are the decay rate of the cavity field and the electron-spin state in the negatively charged NV center, respectively. $\hat{H}$ and $\hat{G}$ are the noise operators. $\hat{a}_{in}$ and $\hat{a}_{out}$ are the input and output vacuum filed operators, respectively. Under the weak excitation ($\langle\hat{\sigma}_z\rangle\approx-1$), the reflection coefficient r_1 of the input photon interacting with the one-sided cavity-NV center system can be described as [61]

$$r_1=\frac{\left[\mathrm{i}(\omega_c-\omega_p)-\frac{\kappa}{2}\right]\left[\mathrm{i}(\omega_t-\omega_p)+\frac{\gamma}{2}\right]+g^2}{\left[\mathrm{i}(\omega_c-\omega_p)+\frac{\kappa}{2}\right]\left[\mathrm{i}(\omega_t-\omega_p)+\frac{\gamma}{2}\right]+g^2}. \tag{3}$$

When the input photon encounters a cold cavity, that is, the coupling strength $g=0$, the reflection coefficient r_0 can be changed into

$$r_0=\frac{\mathrm{i}(\omega_c-\omega_p)-\frac{\kappa}{2}}{\mathrm{i}(\omega_c-\omega_p)+\frac{\kappa}{2}}. \tag{4}$$

Thus in the realistic condition, the state-selective reflection of circularly polarized photon interacting with one-sided cavity-NV center system can be summarized as

$$\begin{aligned}&|0\rangle^p|+1\rangle\rightarrow r_1|0\rangle^p|+1\rangle,\\ &|1\rangle^p|+1\rangle\rightarrow r_0|1\rangle^p|+1\rangle,\\ &|0\rangle^p|-1\rangle\rightarrow r_0|0\rangle^p|-1\rangle,\\ &|1\rangle^p|-1\rangle\rightarrow r_1|1\rangle^p|-1\rangle.\end{aligned} \tag{5}$$

In this section, we will construct a near-unit fidelity and heralded hyper-Toffoli gate based on the above state-selective reflection in Eq. (5). The Toffoli gate completes the function that the target qubit is flipped only when the two control qubits are both in the state $|1\rangle$, there is no operation on the target qubit when the two control qubits is in the state $|0\rangle$. The hyper-Toffoli gate simultaneously performs the Toffoli gate operations on the spatial-polarization DoFs of the three-photon system.

The quantum circuit of the error-detected hyper-Toffoli gate can be divided into two parts. One is used to perform the Toffoli gate operations on the polarized DoF of a three-photon system (shown in Fig. 2) and the other is on spatial DoF (shown in Fig. 3). Here, the building block$_1$ in the green frame interacts with the external cavity-NV$_i$ center systems (i=1, 2). Suppose that the initial states of NV$_1$ and NV$_2$ are both $|-1\rangle$ and the initial polarized and spatial states of three photons are shown as follows:

$$\begin{aligned}&|\phi\rangle_a^p=\alpha_1|0\rangle_a^p+\alpha_2|1\rangle_a^p, \quad |\phi\rangle_a^s=\delta_1|0\rangle_a^s+\delta_2|1\rangle_a^s,\\ &|\phi\rangle_b^p=\beta_1|0\rangle_b^p+\beta_2|1\rangle_b^p, \quad |\phi\rangle_b^s=\epsilon_1|0\rangle_b^s+\epsilon_2|1\rangle_b^s,\\ &|\phi\rangle_c^p=\gamma_1|0\rangle_c^p+\gamma_2|1\rangle_c^p, \quad |\phi\rangle_c^s=\zeta_1|0\rangle_c^s+\zeta_2|1\rangle_c^s.\end{aligned} \tag{6}$$

The coefficients of the same type satisfy the normalized

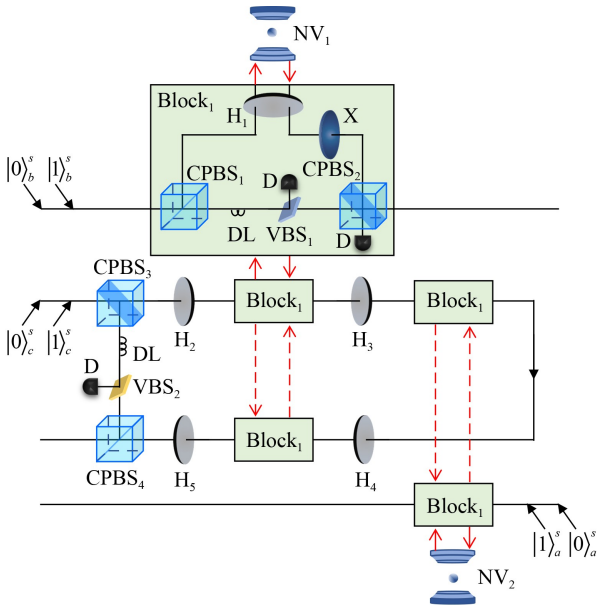

Fig. 2 Schematic diagram for the hyper-parallel Toffoli gate for a three-photon system in polarized DoF assisted by two NV-cavity systems. CPBS$_j$ (j = 1, 2, 3, 4) represents a circularly polarized beam splitter, which completes the reflection of state $|0\rangle^p$ and the transmission of state $|1\rangle^p$. H$_k$ (k = 1, 2, 3, 4, 5) is a half-wave plate inclined at 22.5°, which performs the polarized Hadamard operation, i.e., $|0\rangle^p\rightarrow(|0\rangle^p+|1\rangle^p)/\sqrt{2}, |1\rangle^p\rightarrow(|0\rangle^p-|1\rangle^p)/\sqrt{2}$. X performs a qubit-flip operation on the polarized DoF of a photon $[|0\rangle^p\leftrightarrow|1\rangle^p]$ by tilting the half-wave plate at 45°. VBS$_1$ is an adjustable beam splitter with transmission coefficient $(r_1-r_0)/2$ and reflection coefficient $\sqrt{1-[(r_1-r_0)/2]^2}$. Similarly, the transmission and reflection coefficient of VBS$_2$ are $[(r_1-r_0)/2]^3$ and $\sqrt{1-[(r_1-r_0)/2]^6}$, respectively. D represents a single-photon detector. DL is a delay line, which makes the two wave packets confluent at the same time.

relationship, i.e., $|Y_1|^2+|Y_2|^2=1$ $(Y=\alpha,\ \beta,\ \gamma,\ \delta,\ \epsilon,\ \zeta)$. We will present our proposals in order of function.

In the first part shown in Fig. 2, the Toffoli gate operations are performed on the polarized DoF of three-photon system abc, unaffecting the spatial states of the three photons. First, let the photons a and b simultaneously enter into path $|0\rangle_a^s$ (or $|1\rangle_a^s$) and $|0\rangle_b^s$ (or $|1\rangle_b^s$) from opposite directions, respectively, i.e., photon a interacts with the block$_1$-NV$_2$, meanwhile, photon b interacts with the block$_1$-NV$_1$. In particular, before the two photons a and b pass through block$_1$-NV$_i$ (i=1, 2), the Hadamard operations H_e, i.e., $|+1\rangle\leftrightarrow(|+1\rangle+|-1\rangle)/\sqrt{2}, |-1\rangle\leftrightarrow(|+1\rangle-|-1\rangle)/\sqrt{2}$, are performed on the electron-spin state in NV$_i$ (i=1, 2) center by using a $\pi/2$ femtosecond-level optical pulse [62]. In the block$_1$, the polarized state $|0\rangle^p$ is reflected by the first circularly polarizing beam splitter (CPBS), then it interacts with H$_1$, NV$_i$, H$_1$ and X in sequence, while the polarized state $|1\rangle^p$ is transmitted to a delay line (DL) and an adjustable beam splitter (VBS). After that, the two optical wave packets $|1\rangle^p$ and $|0\rangle^p$ converge on another CPBS$_2$. When all detectors Ds in the block$_1$ are no response, the whole system is transmitted from $|\phi_0\rangle$ into $|\phi_1\rangle$. Here,

$$\begin{aligned}|\phi_0\rangle =&|\phi\rangle_a^p\otimes|\phi\rangle_a^s\otimes|\phi\rangle_b^p\otimes|\phi\rangle_b^s\otimes|\phi\rangle_c^p\otimes|\phi\rangle_c^s\\&\otimes|-1\rangle_1|-1\rangle_2,\\|\phi_1\rangle =&\frac{r_1-r_0}{2\sqrt{2}}[|+1\rangle_2(\alpha_1|0\rangle_a^p+\alpha_2|1\rangle_a^p)\\&+|-1\rangle_2(\alpha_1|0\rangle_a^p-\alpha_2|1\rangle_a^p)]\\&\otimes\frac{r_1-r_0}{2\sqrt{2}}[|+1\rangle_1(\beta_1|0\rangle_b^p+\beta_2|1\rangle_b^p)\\&+|-1\rangle_1(\beta_1|0\rangle_b^p-\beta_2|1\rangle_b^p)]\\&\otimes|\phi\rangle_a^s|\phi\rangle_b^s|\phi\rangle_c^p|\phi\rangle_c^s.\end{aligned}\tag{7}$$

From Eq. (7), the function of block$_1$-NV$_i$ is equal to performing the controlled-phase-flip (CPF) gate operation on the polarized state $|0\rangle^p$ of photon a or b when the electron-spin state are $|-1\rangle$ in NV$_i$ (i=1, 2) centers without affecting its spatial state. When the single-photon detector D in the block$_1$ on the spatial mode $|0\rangle_a^s$ ($|1\rangle_a^s$, $|0\rangle_b^s$, or $|1\rangle_b^s$) responses, it means that the errors originated from the imperfect photon-spin interaction are filtered by CPBS$_2$ and heralded by the D in the block$_1$. That is, the block$_1$ has an error-detected function. After photon a passes through block$_1$-NV$_2$ and photon b passes through block$_1$-NV$_1$, the electron-spin state in NV$_i$ (i=1, 2) centers perform the Hadamard operation H_e again. The quantum state $|\phi_1\rangle$ is changed into $|\phi_{1'}\rangle$,

$$\begin{aligned}|\phi_{1'}\rangle =&\left(\frac{r_1-r_0}{2}\right)^2(\alpha_1|0\rangle_a^p|+1\rangle_2+\alpha_2|1\rangle_a^p|-1\rangle_2)\\&\otimes(\beta_1|0\rangle_b^p|+1\rangle_1+\beta_2|1\rangle_b^p|-1\rangle_1)\\&\otimes|\phi\rangle_a^s|\phi\rangle_b^s|\phi\rangle_c^p|\phi\rangle_c^s.\end{aligned}\tag{8}$$

Second, the photon c is put on the quantum circuit. After the CPBS$_3$, the polarized state $|1\rangle_c^p$ passes through H$_2$, block$_1$-NV$_1$, H$_3$, block$_1$-NV$_2$, H$_4$, block$_1$-NV$_1$ and H$_5$ in sequence, meanwhile, the polarized state $|0\rangle_c^p$ passes through DL and VBS$_2$ with transmission coefficient $[(r_1-r_0)/2]^3$ and reflection coefficient $\sqrt{1-[(r_1-r_0)/2]^6}$. Then the two wave packets cross at another CPBS$_4$ simultaneously by DL. When all detectors Ds in two block$_1$s do not response, the above operations change the quantum state $|\phi_{1'}\rangle$ into

$$\begin{aligned}|\phi_2\rangle =&\left(\frac{r_1-r_0}{2}\right)^5[\alpha_1|0\rangle_a^p|+1\rangle_2(\beta_1\gamma_1|0\rangle_b^p|0\rangle_c^p|+1\rangle_1\\&+\beta_1\gamma_2|0\rangle_b^p|1\rangle_c^p|+1\rangle_1+\beta_2\gamma_1|1\rangle_b^p|0\rangle_c^p|-1\rangle_1\\&+\beta_2\gamma_2|1\rangle_b^p|1\rangle_c^p|-1\rangle_1)\\&+\alpha_2|1\rangle_a^p|-1\rangle_2(\beta_1\gamma_1|0\rangle_b^p|0\rangle_c^p|+1\rangle_1\\&+\beta_1\gamma_2|0\rangle_b^p|1\rangle_c^p|+1\rangle_1+\beta_2\gamma_1|1\rangle_b^p|0\rangle_c^p|-1\rangle_1\\&-\beta_2\gamma_2|1\rangle_b^p|1\rangle_c^p|-1\rangle_1)]\otimes|\phi\rangle_a^s|\phi\rangle_b^s|\phi\rangle_c^s.\end{aligned}\tag{9}$$

Third, we apply Hadamard operations H_e on the two electron-spin states in NV$_1$ and NV$_2$, respectively, and measure them with the basis $\{|+1\rangle,|-1\rangle\}$. If the measurement results of the two-electron-spin states are $|+1\rangle_1$ and $|+1\rangle_2$, the state of the system is changed from $|\phi_2\rangle$ to

$$\begin{aligned}|\phi_3\rangle =&\left(\frac{r_1-r_0}{2}\right)^5[(\alpha_1\beta_1|0\rangle_a^p|0\rangle_b^p+\alpha_1\beta_2|0\rangle_a^p|1\rangle_b^p\\&+\alpha_2\beta_1|1\rangle_a^p|0\rangle_b^p)(\gamma_1|0\rangle_c^p+\gamma_2|1\rangle_c^p)\\&+(\alpha_2\beta_2|1\rangle_a^p|1\rangle_b^p)(\gamma_1|0\rangle_c^p-\gamma_2|1\rangle_c^p)]\\&\otimes|\phi\rangle_a^s|\phi\rangle_b^s|\phi\rangle_c^s,\end{aligned}\tag{10}$$

which is the result of the controlled-controlled-phase-flip (C^{2}PF) gate on the polarized DoF of a three-photon system without affecting its spatial state. That is, when the two electron-spin states in NV$_1$ and NV$_2$ centers, and the polarized states of two photons a and b are $|+1\rangle_1|+1\rangle_2$ and $|1\rangle_a^p|1\rangle_b^p$, the CPF gate operation on the polarized state of photon c. However, the measurement results of the two electron-spin states are other possible outcomes, the corresponding feed-forward single-qubit operations are shown in Table 1. Here, $\sigma_z^p=|0\rangle^p\langle0|-|1\rangle^p\langle1|$ completes the phase-flip operation on polarized state of the photon, and I means keeping its original state. Therefore, the success probability of a

Table 1 The measurement results of the two-electron-spin states in NV$_1$ and NV$_2$, and the corresponding feed-forward single-qubit operations on polarized DoF of three photons.

Measurement results	Single-qubit operations
$\|+1\rangle_1\|+1\rangle_2$	$I_a\otimes I_b\otimes I_c$
$\|+1\rangle_1\|-1\rangle_2$	$(\sigma_z^p)_a\otimes I_b\otimes I_c$
$\|-1\rangle_1\|+1\rangle_2$	$I_a\otimes(\sigma_z^p)_b\otimes I_c$
$\|-1\rangle_1\|-1\rangle_2$	$(\sigma_z^p)_a\otimes(\sigma_z^p)_b\otimes I_c$

C^{2}PF gate on the polarized DoF of a three-photon system is 100% in principle. Finally, before and after the C^{2}PF gate, Hadamard operation performed on the polarized DoF of the target qubit c, i.e., $U^p_{Toffoli} = (H^p \otimes I_4)U^p_{C^2PF}(I_4 \otimes H^p)$, the Toffoli gate on the polarized DoF of the three-photon system is finished without impacting on the spatial DoF of the three-photon system. Here,

$$\begin{aligned}|\phi_4\rangle = &\left(\frac{r_1 - r_0}{2}\right)^5 [(\alpha_1\beta_1|0\rangle^p_a|0\rangle^p_b + \alpha_1\beta_2|0\rangle^p_a|1\rangle^p_b \\ &+ \alpha_2\beta_1|1\rangle^p_a|0\rangle^p_b)(\gamma_1|0\rangle^p_c + \gamma_2|1\rangle^p_c) \\ &+ (\alpha_2\beta_2|1\rangle^p_a|1\rangle^p_b)(\gamma_1|1\rangle^p_c + \gamma_2|0\rangle^p_c)] \\ &\otimes |\phi\rangle^s_a|\phi\rangle^s_b|\phi\rangle^s_c. \end{aligned} \tag{11}$$

In next part shown in Fig. 3, the Toffoli gate operations, are performed on the spatial DoF of three-photon, by utilizing two cavity-NV systems and five block$_2$ to finish system abc, without changing the polarized states of three photons. Suppose that the states of the three photons are the same as ones described in Eq. (6), and meanwhile the states of NV_3 and NV_4 are $|+1\rangle_3$ and $|-1\rangle_4$, respectively.

First, after the Hadamard operations H_e are performed on the two electron-spin states in NV_3 and NV_4, let the photons a and b simultaneously enter into path $|0\rangle^s_a$ (or $|1\rangle^s_a$) and $|0\rangle^s_b$ (or $|1\rangle^s_b$) from opposite directions, respectively. In detail, photon a from the spatial path $|1\rangle^s_a$ interacts with the block$_2$-NV_4, meanwhile, photon b from the spatial path $|1\rangle^s_b$ interacts with the block$_2$-NV_3. Both photon a from the spatial path $|0\rangle^s_a$ and photon b from the spatial path $|0\rangle^s_b$ pass through a VBS_1 and a DL in sequence. VBS_1 is used to adjust the transmission coefficient. DL is used to make the two paths $|0\rangle^s_a$ and $|1\rangle^s_a$, and $|0\rangle^s_b$ and $|1\rangle^s_b$ of two photons a and b arrive simultaneously. In the block$_2$-NV_3, the polarized state $|0\rangle^p$ of photon b is reflected by $CPBS_1$, then it sequentially passes through H_1, NV_3, and H_1, while the polarized state $|1\rangle^p$ is transmitted to sequentially pass through X_1, H_1, NV_3, H_1, and X_2. After that, the two optical wave packets converge on another $CPBS_2$. So does the photon a in the block$_2$-NV_4. When all detectors Ds in the block$_2$ and VBS_1s are no response, the state of the whole system is transmitted from $|\psi_0\rangle$ into $|\psi_1\rangle$. Here,

$$\begin{aligned}|\psi_0\rangle = &|\phi\rangle^p_a \otimes |\phi\rangle^s_a \otimes |\phi\rangle^p_b \otimes |\phi\rangle^s_b \otimes |\phi\rangle^p_c \otimes |\phi\rangle^s_c \\ &\otimes |+1\rangle_3 \otimes |-1\rangle_4, \\ |\psi_1\rangle = &\frac{r_1 - r_0}{2\sqrt{2}}[|+1\rangle_4(\delta_1|0\rangle_a + \delta_2|1\rangle_a) \\ &+ |-1\rangle_4(-\delta_1|0\rangle_a + \delta_2|1\rangle_a)] \\ &\otimes \frac{r_1 - r_0}{2\sqrt{2}}[|+1\rangle_3(\epsilon_1|0\rangle^s_b + \epsilon_2|1\rangle^s_b) \\ &+ |-1\rangle_3(\epsilon_1|0\rangle^s_b - \epsilon_2|1\rangle^s_b)] \\ &\otimes |\phi\rangle^p_a|\phi\rangle^p_b|\phi\rangle^p_c|\phi\rangle^s_c. \end{aligned} \tag{12}$$

From Eq. (12), the function of block$_2$-NV_j ($j = 3, 4$) is equal to performing the CPF gate operation on the spatial state $|0\rangle^s$ of photon a or b when the electron-spin state $|-1\rangle$ in NV_j ($j = 3, 4$) center, without affecting its polarized state. Similarly, when the detector D in the block$_2$ on the spatial mode $|1\rangle^s_a$ ($|1\rangle^s_b$) or VBS_1 on the spatial mode $|0\rangle^s_a$ ($|0\rangle^s_b$) responses, the errors caused by the imperfect photon scattering are heralded by the D. That is, the block$_2$ also has an error-detected function. After the photons a from the spatial path $|1\rangle^s_a$ and b from the spatial path $|1\rangle^s_b$ interact with block$_2$-NV_4 and block$_2$-NV_3, respectively, the two electron-spin states in NV_3 and NV_4 centers perform the Hadamard operations H_e again. The quautum state $|\psi_1\rangle$ is changed into $|\psi_{1'}\rangle$,

$$\begin{aligned}|\psi_{1'}\rangle = &\left(\frac{r_1 - r_0}{2}\right)^2 (\delta_1|0\rangle^s_a|-1\rangle_4 + \delta_2|1\rangle^s_a|+1\rangle_4) \\ &\otimes (\epsilon_1|0\rangle^s_b|+1\rangle_3 + \epsilon_2|1\rangle^s_b|-1\rangle_3) \\ &\otimes |\phi\rangle^p_a|\phi\rangle^p_b|\phi\rangle^p_c|\phi\rangle^s_c. \end{aligned} \tag{13}$$

Second, the photon c is put the quantum circuit. The photon c from the spatial state $|0\rangle^s_c$ passes through a VBS_1 and a DL in sequence. After the photon c from the spatial path $|1\rangle^s_c$ passes through BS_1, it completes the transformation, i.e., $|1\rangle^s_c \leftrightarrow (|0\rangle^s_d + |1\rangle^s_d)/\sqrt{2}$. Subsequently, the photon c from the spatial path $|1\rangle^s_d$ passes through

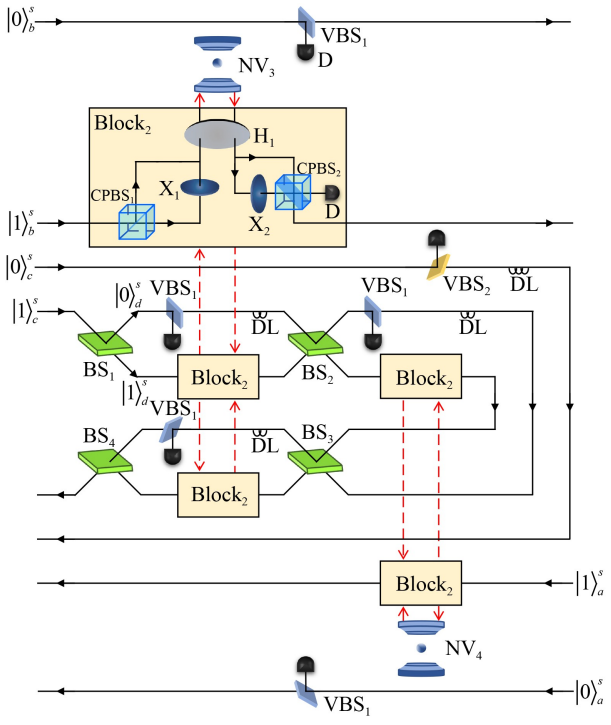

Fig. 3 Schematic diagram for the hyper-parallel Toffoli gate for a three-photon system in spatial DoF assisted by two NV-microcavity systems. BS_1 and BS_4 denote 50:50 beam splitter which completes the Hadamard operation of the photon in spatial DoF, i.e., $|1\rangle^s_c \leftrightarrow (|0\rangle^s_d + |1\rangle^s_d)/\sqrt{2}$. BS_2 and BS_3 complete the operation, i.e., $|0\rangle^s_d \leftrightarrow (|0\rangle^s_d + |1\rangle^s_d)/\sqrt{2}, |1\rangle^s_d \leftrightarrow (|0\rangle^s_d - |1\rangle^s_d)/\sqrt{2}$.

block$_2$-NV$_3$, BS$_2$, block$_2$-NV$_4$, BS$_3$, DL, VBS$_1$ in sequence, while the photon c from the spatial path $|0\rangle_d^s$ passes through VBS$_1$, DL, BS$_2$, VBS$_1$, DL, BS$_3$, block$_2$-NV$_3$ in sequence. Then the photon c from the spatial path $|0\rangle_d^s$ and $|1\rangle_d^s$ converge at BS$_4$. Here, BS$_k$ (k=2,3) is used to completes the Hadamard operation on the spatial DoF of the photon c, i.e., $|0\rangle_d^s \leftrightarrow (|0\rangle_d^s + |1\rangle_d^s)/\sqrt{2}$, and $|1\rangle_d^s \leftrightarrow (|0\rangle_d^s - |1\rangle_d^s)/\sqrt{2}$. DLs are used to make two spatial paths $|0\rangle_d^s$ and $|1\rangle_d^s$ of the photon c converge at simultaneously BS$_2$, BS$_3$, and BS$_4$, respectively. DLs from the spatial paths $|0\rangle_a^s$, and $|0\rangle_b^s$, $|0\rangle_c^s$ make the photons a, b, and c arrive simultaneously, respectively. When all detectors Ds in three block$_2$s, VBS$_1$s and VBS$_2$s do not response, the above operations change the quautum state $|\psi_{1'}\rangle$ into

$$\begin{aligned}|\psi_2\rangle = \left(\frac{r_1 - r_0}{2}\right)^5 & [(\delta_1\epsilon_1|0\rangle_a^s|0\rangle_b^s + \delta_1\epsilon_2|0\rangle_a^s|1\rangle_b^s \\ & + \delta_2\epsilon_1|1\rangle_a^s|0\rangle_b^s)(\zeta_1|0\rangle_c^s + \zeta_2|1\rangle_c^s) \\ & + (\delta_2\epsilon_2|1\rangle_a^s|1\rangle_b^s)(\zeta_1|0\rangle_c^s - \zeta_2|1\rangle_c^s)] \\ & \otimes |\phi\rangle_a^p|\phi\rangle_b^p|\phi\rangle_c^p. \end{aligned} \tag{14}$$

Third, we apply Hadamard operations H$_e$ on the two electron-spin states in NV$_3$ and NV$_4$ centers, respectively, and measure them with the basis $\{|+1\rangle, |-1\rangle\}$. If the measurement results of the two electron-spin states are $|+1\rangle_1$ and $|+1\rangle_2$, the state of the system is changed from $|\psi_2\rangle$ to

$$\begin{aligned}|\psi_3\rangle = \left(\frac{r_1 - r_0}{2}\right)^5 & [(\delta_1\epsilon_1|0\rangle_a^s|0\rangle_b^s + \delta_1\epsilon_2|0\rangle_a^s|1\rangle_b^s \\ & + \delta_2\epsilon_1|1\rangle_a^s|0\rangle_b^s)(\zeta_1|0\rangle_c^s + \zeta_2|1\rangle_c^s) \\ & + \delta_2\epsilon_2|1\rangle_a^s|1\rangle_b^s(\zeta_1|0\rangle_c^s - \zeta_2|1\rangle_c^s)] \\ & \otimes |\phi\rangle_a^p|\phi\rangle_b^p|\phi\rangle_c^p, \end{aligned} \tag{15}$$

which is the result of the C^{2}PF gate on the spatial DoF of the three-photon system without affecting its polarized state. That is, when the two electron-spin states in NV$_3$ and NV$_4$, and the polarized states of two photons ab are $|+1\rangle_3|+1\rangle_4$ and $|1\rangle_a^s|1\rangle_b^s$, the CPF gate operates on the spatial state of photon c. However, the measurement results of the two-electron-spin states are other possible outcomes, the corresponding feed-forward single-qubit operations are shown in Table 2. Here, phase shifter $e^{i\pi}$, which completes the transformation $|0\rangle^p \to -|0\rangle^p$ and $|1\rangle^p \to -|1\rangle^p$, is performed on spatial state, and I means keeping its original state. Therefore, the success probability of a C^{2}PF gate on the spatial DoF of a three-photon system is 100% in principle. Finally, before and after the C^{2}PF gate, Hadamard operation is performed on the spatial DoF of the target qubit c, i.e., $U_{Toffoli}^s = (H^s \otimes I_4)U_{C^2PF}^s(I_4 \otimes H^s)$, the Toffoli gate on the spatial DoF of the three-photon system is finished without impacting on the polarized DoF of the three-photon system. Here,

$$\begin{aligned}|\psi_4\rangle = \left(\frac{r_1 - r_0}{2}\right)^5 & [(\delta_1\epsilon_1|0\rangle_a^s|0\rangle_b^s + \delta_1\epsilon_2|0\rangle_a^s|1\rangle_b^s \\ & + \delta_2\epsilon_1|1\rangle_a^s|0\rangle_b^s)(\zeta_1|0\rangle_c^s + \zeta_2|1\rangle_c^s) \\ & + \delta_2\epsilon_2|1\rangle_a^s|1\rangle_b^s(\zeta_2|0\rangle_c^s + \zeta_1|1\rangle_c^s)] \\ & \otimes |\phi\rangle_a^p|\phi\rangle_b^p|\phi\rangle_c^p. \end{aligned} \tag{16}$$

Finally, we can combine the above two parts in Figs. 2 and 3 to construct an error-detected hyper-parallel Toffoli gate with state-selective reflection, as the Toffoli gates of the three-photon system in the polarized and spatial DoFs are independent of each other. The hybrid quantum CPF gate operations are the key elements of this hyper-Toffoli gate. The above two Tables 1 and 2 are also valid when the four electron spins of the NV-cavity systems are in other states. Thus, our error-detected hyper-parallel Toffoli gate is very flexible. Here,

$$\begin{aligned}|\Phi\rangle = \left(\frac{r_1 - r_0}{2}\right)^5 & [(\alpha_1\beta_1|0\rangle_a^p|0\rangle_b^p + \alpha_1\beta_2|0\rangle_a^p|1\rangle_b^p \\ & + \alpha_2\beta_1|1\rangle_a^p|0\rangle_b^p)(\gamma_1|0\rangle_c^p + \gamma_2|1\rangle_c^p) \\ & + (\alpha_2\beta_2|1\rangle_a^p|1\rangle_b^p)(\gamma_1|1\rangle_c^p + \gamma_2|0\rangle_c^p)] \\ & \otimes \left(\frac{r_1 - r_0}{2}\right)^5 [(\delta_1\epsilon_1|0\rangle_a^s|0\rangle_b^s + \delta_1\epsilon_2|0\rangle_a^s|1\rangle_b^s \\ & + \delta_2\epsilon_1|1\rangle_a^s|0\rangle_b^s)(\zeta_1|0\rangle_c^s + \zeta_2|1\rangle_c^s) \\ & + (\delta_2\epsilon_2|1\rangle_a^s|1\rangle_b^s)(\zeta_1|1\rangle_c^s + \zeta_2|0\rangle_c^s)]. \end{aligned} \tag{17}$$

As the incomplete and imperfect cavity-NV-center interactions are transformed into the detectable failure rather than infidelity based on the novel heralding mechanism of detectors in the block$_1$ and block$_2$, our hyper-Toffoli gate of the three-photon system is error-detected. The efficiencies of the two blocks can be further improved by repeating the operation processes when the detectors in blocks are clicked. Now, we have obtained the result of the error-detected hyper-parallel Toffoli gate with state-selective reflection of one-sided cavity-NV center system. That is, when the polarized state of two photons ab are $|1\rangle_a^p|1\rangle_b^p$, the polarized states of the photon c is flipped; when the spatial state of two photons ab are $|1\rangle_a^s|1\rangle_b^s$, the spatial states of the photon c is flipped. No operation is performed on the photon c when the polarized state of two photons ab are $|0\rangle_a^p|0\rangle_b^p$ ($|0\rangle_a^p|1\rangle_b^p$ or $|1\rangle_a^p|0\rangle_b^p$) and the spatial state of two photons ab are $|0\rangle_a^s|0\rangle_b^s$ ($|0\rangle_a^s|1\rangle_b^s$ or $|1\rangle_a^s|0\rangle_b^s$).

Table 2 The measurement results of the two-electron-spin states in NV$_3$ and NV$_4$, and the corresponding feed-forward single-qubit operations on polarized DoF of three photons.

Measurement results	Single-qubit operations
$\|+1\rangle_3\|+1\rangle_4$	$I_a \otimes I_b \otimes I_c$
$\|+1\rangle_3\|-1\rangle_4$	$e^{i\pi}\|0\rangle_a^s \otimes I_b \otimes I_c$
$\|-1\rangle_3\|+1\rangle_4$	$I_a \otimes e^{i\pi}\|1\rangle_b^s \otimes I_c$
$\|-1\rangle_3\|-1\rangle_4$	$e^{i\pi}\|0\rangle_a^s \otimes e^{i\pi}\|1\rangle_b^s \otimes I_c$

3 Discussion and conclusion

In this work, we have designed an error-detected quantum circuit for implementing the hyper-parallel Toffoli gate on a three-photon system in both the polarization and spatial DoFs, assisted by state-selective reflection of one-sided cavity-NV-center system. The hyper-Toffoli gate can perform double Toffoli gate operations on only one three-photon system in two DoFs with four one-sided cavity-NV center systems, which can save the resource depletion and decrease the photonic dispassion noise in QIP. The interaction of the photons is accomplished by the photon–electron–spin interaction in the NV center, which can be greatly improve by coupled to an optical cavity, fiber-based microcavity or microring resonator either in strong coupling regime and in weak coupling regime in experiment [41–44, 63–65]. The identically optical transition of the four uncorrelated NV centers, can be achieved by applying controlled external electric fields [66, 67]. Our schemes are nearly immune to spectral diffusion and charge fluctuation because of the narrow linewidth of the state $|A_2\rangle$ [52]. Many techniques have been explored to reduce and eliminate the spectral-diffusion influence [45–47, 68].

We can also construct three types of flexible hybrid hyper-Toffoli gate assisted by the state-selective reflection of one-sided cavity-NV-center system. The quantum circuit of the hybrid hyper-Toffoli gates in Fig. 4 is similar to the one of the hyper-Toffoli gate in Fig. 2 and Fig. 3, by replacing H and block$_1$ with BS and block$_2$, respectively. As shown in Fig. 4, we construct a hybrid hyper-Toffoli gate, that is, the polarized (spatial) states of two photons a and b to control the spatial (polarized) state of photon c, respectively. In detail, if all Ds cannot click of Fig. 4(a), the quantum circuit finishes the polarized states of two photons a and b to control the spatial state of photon c. Here,

$$\begin{aligned}|\phi_h\rangle = &\left(\frac{r_1 - r_0}{2}\right)^5 [(\alpha_1\beta_1|0\rangle_a^p|0\rangle_b^p + \alpha_1\beta_2|0\rangle_a^p|1\rangle_b^p \\ &+ \alpha_2\beta_1|1\rangle_a^p|0\rangle_b^p)(\zeta_1|0\rangle_c^s + \zeta_2|1\rangle_c^s) \\ &+ (\alpha_2\beta_2|1\rangle_a^p|1\rangle_b^p)(\zeta_1|1\rangle_c^s + \zeta_2|0\rangle_c^s)] \\ &\otimes |\phi\rangle_a^s|\phi\rangle_b^s|\phi\rangle_c^p. \end{aligned} \tag{18}$$

If all Ds in Fig. 4(b) cannot click, the quantum circuit completes that the spatial states of two photons a and b control the polarized state of photon c. Here,

$$\begin{aligned}|\phi_t\rangle = &\left(\frac{r_1 - r_0}{2}\right)^5 [(\delta_1\epsilon_1|0\rangle_a^s|0\rangle_b^s + \delta_1\epsilon_2|0\rangle_a^s|1\rangle_b^s \\ &+ \delta_2\epsilon_1|1\rangle_a^s|0\rangle_b^s)(\gamma_1|0\rangle_c^p + \gamma_2|1\rangle_c^p) \\ &+ (\delta_2\epsilon_2|1\rangle_a^s|1\rangle_b^s)(\gamma_1|1\rangle_c^p + \gamma_2|0\rangle_c^p)] \\ &\otimes |\phi\rangle_a^p|\phi\rangle_b^p|\phi\rangle_c^s. \end{aligned} \tag{19}$$

Obviously, we can unite the two parts to achieve a hybrid hyper-paralleled Toffoli gate with state-selective reflection. Here,

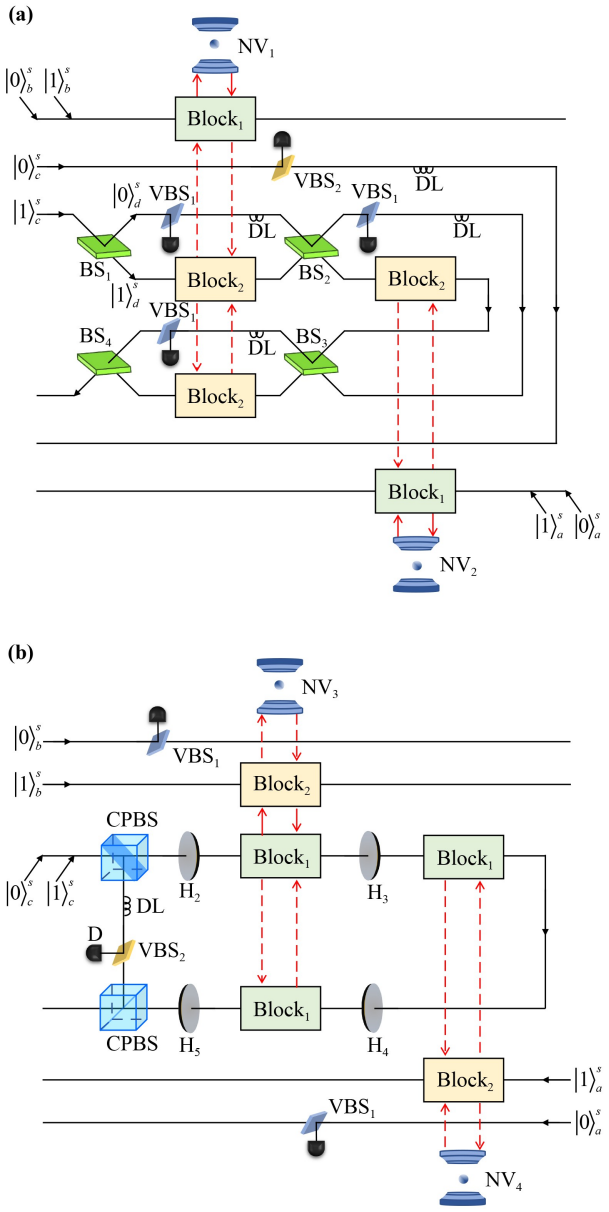

Fig. 4 Schematic diagram of a hybrid hyper-Toffoli gate.

$$\begin{aligned}|\Phi_1\rangle = &\left(\frac{r_1 - r_0}{2}\right)^5 [(\alpha_1\beta_1|0\rangle_a^p|0\rangle_b^p + \alpha_1\beta_2|0\rangle_a^p|1\rangle_b^p \\ &+ \alpha_2\beta_1|1\rangle_a^p|0\rangle_b^p)(\zeta_1|0\rangle_c^s + \zeta_2|1\rangle_c^s) \\ &+ (\alpha_2\beta_2|1\rangle_a^p|1\rangle_b^p)(\zeta_1|1\rangle_c^s + \zeta_2|0\rangle_c^s)] \\ &\otimes (\frac{r_1 - r_0}{2})^5[(\delta_1\epsilon_1|0\rangle_a^s|0\rangle_b^s + \delta_1\epsilon_2|0\rangle_a^s|1\rangle_b^s \\ &+ \delta_2\epsilon_1|1\rangle_a^s|0\rangle_b^s)(\gamma_1|0\rangle_c^p + \gamma_2|1\rangle_c^p) \\ &+ (\delta_2\epsilon_2|1\rangle_a^s|1\rangle_b^s)\,(\gamma_1|1\rangle_c^p + \gamma_2|0\rangle_c^p)]. \end{aligned} \tag{20}$$

Similarly, we can also construct other types of flexible hybrid hyper-Toffoli gate assisted by the state-selective reflection of one-sided cavity-NV-center system. For

example, the polarized (spatial) states of photon a and the spatial (polarized) states of photon b control the spatial (polarized) state of photon c, respectively. Here,

$$
\begin{aligned}
|\Phi_2\rangle = & \left(\frac{r_1 - r_0}{2}\right)^5 [(\alpha_1\epsilon_1|0\rangle_a^p|0\rangle_b^s + \alpha_1\epsilon_2|0\rangle_a^p|1\rangle_b^s \\
& + \alpha_2\epsilon_1|1\rangle_a^p|0\rangle_b^s)(\zeta_1|0\rangle_c^s + \zeta_2|1\rangle_c^s) \\
& + (\alpha_2\epsilon_2|1\rangle_a^p|1\rangle_b^s)(\zeta_1|1\rangle_c^s + \zeta_2|0\rangle_c^s)] \\
& \otimes \left(\frac{r_1 - r_0}{2}\right)^5 [(\delta_1\beta_1|0\rangle_a^s|0\rangle_b^p + \delta_1\beta_2|0\rangle_a^s|1\rangle_b^p \\
& + \delta_2\beta_1|1\rangle_a^s|0\rangle_b^p)(\gamma_1|0\rangle_c^p + \gamma_2|1\rangle_c^p) \\
& + (\delta_2\beta_2|1\rangle_a^s|1\rangle_b^p)(\gamma_1|1\rangle_c^p + \gamma_2|0\rangle_c^p)], \\
|\Phi_3\rangle = & \left(\frac{r_1 - r_0}{2}\right)^5 [(\alpha_1\epsilon_1|0\rangle_a^p|0\rangle_b^s + \alpha_1\epsilon_2|0\rangle_a^p|1\rangle_b^s \\
& + \alpha_2\epsilon_1|1\rangle_a^p|0\rangle_b^s)(\gamma_1|0\rangle_c^p + \gamma_2|1\rangle_c^p) \\
& + (\alpha_2\beta_2|1\rangle_a^p|1\rangle_b^p)(\gamma_1|1\rangle_c^p + \gamma_2|0\rangle_c^p)] \\
& \otimes \left(\frac{r_1 - r_0}{2}\right)^5 [(\delta_1\beta_1|0\rangle_a^s|0\rangle_b^p + \delta_1\beta_2|0\rangle_a^s|1\rangle_b^p \\
& + \delta_2\beta_1|1\rangle_a^s|0\rangle_b^p)(\zeta_1|0\rangle_c^s + \zeta_2|1\rangle_c^s) \\
& + (\delta_2\epsilon_2|1\rangle_a^s|1\rangle_b^s)(\zeta_1|1\rangle_c^s + \zeta_2|0\rangle_c^s)].
\end{aligned}
\tag{21}
$$

In the above protocols, we have taken into account practical experiment environment, including the cavity leakage rate and the coupling strength. The probability η_D^p of D triggered in the block$_1$ and the one η_D^s in the block$_2$ is equal to $\eta_D^p = \eta_D^s = \eta_D = (\frac{r_1+r_0}{2})^2$, in Fig. 5, which are related to the coupling strength g, cavity decay and leakage rate κ, γ at $\gamma = 0.01\kappa$. Obviously, the probability η_D shown in Table 3 exists zero values even in the weak coupling rate, which results from the destructive interference. Therefore, the fidelity of the hyper-Toffoli gates is unity in principle without strong couple limitation between photon and NV center. These positive characteristics may make our projects conducive to increase the information processing capability and decrease the complexity of large-scale integration. The efficiency of the hyper-Toffoli gates is $\eta_T = (\frac{r_1-r_0}{2})^{10}$, the ratio of the number of output photons to the input. The relation between η_T and g/κ is shown in Fig. 5 and the partial detailed data is shown in Table 3. One can see that our schemes can work not only in strong coupling rate but also in the weak coupling rate. To achieve a higher efficiency η_T, γ/κ should be as small as possible, which can be realized by improving the design and manufacturing process of cavity. Besides, the efficiency of our scheme can also reduced from non-ideal single-photon sources, imperfect linear-optical elements (BSs and CPBSs), and invalid dark detectors, which will be improved with the further development of the current technology.

In summary, we have proposed an error-detected hyper-Toffoli gate for the three-photon system based on the interface between polarized photon and cavity-NV-center system. This hyper-Toffoli gate is equivalent to performing double Toffoli gate operations simultaneously on both the polarization and spatial DoFs of the three-photon system with a low decoherence, short operation time, and less quantum resources required, in compared with those on two independent three-photon systems in one DoF only. Based on the heralding mechanism of detectors, the imperfect interactions between the cavity-NV center and the photon can be translated into judging the response status of the detectors, so the fidelity of our proposal is near unity. The efficiency of our optimal protocol for the hyper-Toffoli gate can be improved further by repeating the operation processes when the detectors are clicked. We can also construct three types of hybrid hyper-Toffoli gate assisted by the state-selective reflection of one-sided cavity-NV-center system, as the quantum circuit of the hyper-Toffoli gate is flexible and adjustable. Besides, the modular circuits effectively reduce the complexity of Toffoli gate, and beyond that, two photons enter the systems simultaneously from opposite directions can effectively reduce the overall running time. Moreover, the evaluation of gate performance with achieved experiment parameters, even in the weak coupling, shows that it is feasible with current experimental technology and provides a promising building block for quantum compute.

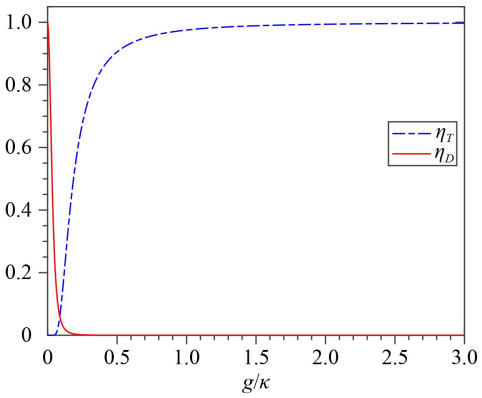

Fig. 5 The efficiency η_T of the hyper-Toffoli gates and the probability η_D of D triggered in the block$_1$ vs the ratio of g/κ when $\omega_c = \omega_p = \omega_c$ at $\gamma = 0.01\kappa$.

Table 3 The efficiency η_T of the hyper-Toffoli gates and the probability η_D of D triggered in the block$_1$ or block$_2$ vs. the ratio of g/κ when $\omega_c = \omega_p = \omega_c$ at $\gamma = 0.01\kappa$.

	$g/\kappa = 0.5$	$g/\kappa = 1.5$	$g/\kappa = 2.4$
η_T	90.53%	98.90%	99.57%
η_D	0.01%	0	0

Acknowledgements This work was supported in part by the National Natural Science Foundation of China under Contract 61901420, the Shanxi Province Science Foundation for Youths under

Contract 201901D211235, the Scientific and Technological Innovation Programs of Higher Education Institutions in Shanxi under Contract 2019L0507, and the Shanxi "1331 Project" Key Subjects Construction.

References

1. M. A. Nielsen, I. Chuang, and L. K. Grover, Quantum computation and quantum information, *Am. J. Phys.* 70(5), 558 (2002)
2. L. X. Liang, Y. Y. Zheng, Y. X. Zhang, and M. Zhang, Error-detected *N*-photon cluster state generation based on the controlled-phase gate using a quantum dot in an optical microcavity, *Front. Phys.* 15(2), 21601 (2020)
3. T. Li and G. L. Long, Quantum secure direct communication based on single-photon Bell-state measurement, *New J. Phys.* 22(6), 063017 (2020)
4. Z. D. Ye, D. Pan, Z. Sun, C. G. Du, L. G. Yin, and G. L. Long, Generic security analysis framework for quantum secure direct communication, *Front. Phys.* 16(2), 21503 (2021)
5. P. S. Yan, L. Zhou, W. Zhong, and Y. B. Sheng, Measurement-based entanglement purification for entangled coherent states, *Front. Phys.* 17(2), 21501 (2022)
6. C. Wang, Quantum secure direct communication: Intersection of communication and cryptography, *Fundam. Res.* 1(1), 91 (2021)
7. P. Wang, C. Q. Yu, Z. X. Wang, R. Y. Yuan, F. F. Du, and B. C. Ren, Hyperentanglement-assisted hyperdistillation for hyper-encoding photon system, *Front. Phys.* 17(3), 31501 (2022)
8. P. W. Shor, Polynomial-time algorithms for prime factorization and discrete logarithms on a quantum computer, *SIAM Rev.* 41(2), 303 (1999)
9. L. K. Grover, Quantum mechanics helps in searching for a needle in a haystack, *Phys. Rev. Lett.* 79(2), 325 (1997)
10. M. AbuGhanem, A. H. Homid, and M. Abdel-Aty, Cavity control as a new quantum algorithms implementation treatment, *Front. Phys.* 13(1), 130303 (2018)
11. X. D. Cai, D. Wu, Z. E. Su, M. C. Chen, X. L. Wang, L. Li, N. L. Liu, C. Y. Lu, and J. W. Pan, Entanglement-based machine learning on a quantum computer, *Phys. Rev. Lett.* 114(11), 110504 (2015)
12. J. Allcock and S. Y. Zhang, Quantum machine learning, *Natl. Sci. Rev.* 6(1), 26 (2019)
13. X. L. Ouyang, X. Z. Huang, Y. K. Wu, W. G. Zhang, X. Wang, H. L. Zhang, L. He, X. Y. Chang, and L. M. Duan, Experimental demonstration of quantum-enhanced machine learning in a nitrogen-vacancy-center system, *Phys. Rev. A* 101(1), 012307 (2020)
14. D. R. Chong, M. Kim, J. Ahn, and H. Jeong, Machine learning identification of symmetrized base states of Rydberg atoms, *Front. Phys.* 17(1), 12504 (2022)
15. W. Q. Liu and H. R. Wei, Optimal synthesis of the Fredkin gate in a multilevel system, *New J. Phys.* 22(6), 063026 (2020)
16. W. Q. Liu, H. R. Wei, and L. C. Kwek, Low-cost Fredkin gate with auxiliary space, *Phys. Rev. A* 14(5), 054057 (2020)
17. V. V. Shende, I. L. Markov, and S. S. Bullock, Minimal universal two-qubit controlled-NOT-based circuits, *Phys. Rev. A* 69(6), 062321 (2004)
18. T. C. Ralph, K. J. Resch, and A. Gilchrist, Efficient Toffoli gates using qudits, *Phys. Rev. A* 75(2), 022313 (2007)
19. I. Radu, T. P. Spiller, and W. J. Munro, Generalized Toffoli gates using qudit catalysis, *Phys. Rev. A* 80(1), 012313 (2009)
20. N. K. Yu, R. Y. Duan, and M. S. Ying, Five two-qubit gates are necessary for implementing the Toffoli gate, *Phys. Rev. A* 88(1), 010304 (2013)
21. J. Fiurášek, Linear-optics quantum Toffoli and Fredkin gates, *Phys. Rev. A* 73(6), 062313 (2006)
22. M. Soeken, D. M. Miller, and R. Drechsler, Quantum circuits employing roots of the Pauli matrices, *Phys. Rev. A* 88(4), 042322 (2013)
23. A. Fedorov, L. Steffen, M. Baur, M. P. da Silva, and A. Wallraff, Implementation of a Toffoli gate with superconducting circuits, *Nature* 481(7380), 170 (2012)
24. S. E. Rasmussen, K. Groenland, R. Gerritsma, K. Schoutens, and N. T. Zinner, Single-step implementation of high-fidelity *n*-bit Toffoli gatess, *Phys. Rev. A* 101(2), 022308 (2020)
25. S. Daraeizadeh, S. P. Premaratne, N. Khammassi, X. Song, M. Perkowski, and A. Y. Matsuura, Machine learning-based three-qubit gate design for the Toffoli gate and parity check in transmon systems, *Phys. Rev. A* 102(1), 012601 (2020)
26. H. R. Wei and F. G. Deng, Compact quantum gates on electron-spin qubits assisted by diamond nitrogen vacancy centers inside cavities, *Phys. Rev. A* 88(4), 042323 (2013)
27. H. R. Wei and F. G. Deng, Scalable quantum computing based on stationary spin qubits in coupled quantum dots inside double-sided optical microcavities, *Sci. Rep.* 4(1), 7551 (2015)
28. H. R. Wei and F. G. Deng, Universal quantum gates on electron-spin qubits with quantum dots inside single-side optical microcavities, *Opt. Express* 22(1), 593 (2014)
29. G. Z. Song, J. L. Guo, Q. Liu, H. R. Wei, and G. L. Long, Heralded quantum gates for hybrid systems via waveguide-mediated photon scattering, *Phys. Rev. A* 104(1), 012608 (2021)
30. T. Monz, K. Kim, W. Hänsel, M. Riebe, A. S. Villar, P. Schindler, M. Chwalla, M. Hennrich, and R. Blatt, Realization of the quantum Toffoli gate with trapped ions, *Phys. Rev. Lett.* 102(4), 040501 (2009)
31. D. Solenov, S. E. Economou, and T. L. Reinecke, Fast two-qubit gates for quantum computing in semiconductor quantum dots using a photonic microcavity, *Phys. Rev. B* 87(3), 035308 (2013)
32. B. P. Lanyon, M. Barbieri, M. P. Almeida, T. Jennewein, T. C. Ralph, K. J. Resch, G. J. Pryde, J. L. O'Brien, A. Gilchrist, and A. G. White, Simplifying quantum logic using higher-dimensional Hilbert spaces, *Nat. Phys.* 5(2), 134 (2009)
33. E. O. Kiktenko, A. S. Nikolaeva, P. Xu, G. V. Shlyapnikov, and A. K. Fedorov, Scalable quantum computing with qudits on a graph, *Phys. Rev. A* 101(2), 022304

(2020)
34. T. Li and G. L. Long, Hyperparallel optical quantum computation assisted by atomic ensembles embedded in double-sided optical cavities, *Phys. Rev. A* 94(2), 022343 (2016)
35. Y. H. Han, C. Cao, L. Fan, and R. Zhang, Heralded high-fidelity quantum hyper-CNOT gates assisted by charged quantum dots inside single-sided optical microcavities, *Opt. Express* 29(13), 20045 (2021)
36. F. F. Du and Z. R. Shi, Robust hybrid hyper-controlled-not gates assisted by an input—output process of low-Q cavities, *Opt. Express* 27(13), 17493 (2019)
37. H. R. Wei and G. L. Long, Universal photonic quantum gates assisted by ancilla diamond nitrogen-vacancy centers coupled to resonators, *Phys. Rev. A* 91(3), 032324 (2015)
38. T. J. Wang, Y. Zhang, and C. Wang, Universal hybrid hyper-controlled quantum gates assisted by quantum dots in optical double-sided microcavities, *Laser Phys. Lett.* 11(2), 025203 (2014)
39. H. R. Wei, F. G. Deng, and G. L. Long, Hyper-parallel Toffoli gate on three-photon system with two degrees of freedom assisted by single-sided optical microcavities, *Opt. Express* 24(16), 18619 (2016)
40. S. H. Ru, Y. L. Wang, M. An, F. R. Wang, P. Zhang, and F. L. Li, Realization of a deterministic quantum Toffoli gate with a single photon, *Phys. Rev. A* 103(2), 022606 (2021)
41. T. Gaebel, M. Domhan, I. Popa, C. Wittmann, P. Neumann, F. Jelezko, J. R. Rabeau, N. Stavrias, A. D. Greentree, S. Prawer, J. Meijer, J. Twamley, P. R. Hemmer, and J. Wrachtrup, Room-temperature coherent coupling of single spins in diamond, *Nat. Phys.* 2(6), 408 (2006)
42. G. D. Fuchs, V. V. Dobrovitski, D. M. Toyli, F. J. Heremans, and D. D. Awschalom, Gigahertz dynamics of a strongly driven single quantum spin, *Science* 326(5959), 1520 (2009)
43. D. Englund, B. Shields, K. Rivoire, F. Hatami, J. Vučković, H. Park, and M. D. Lukin, Deterministic coupling of a single nitrogen vacancy center to a photonic crystal cavity, *Nano Lett.* 10(10), 3922 (2010)
44. J. Zhang, and D. Suter, Experimental Protection of Two-Qubit Quantum Gates against Environmental Noise by Dynamical Decoupling, *Phys. Rev. Lett.* 115(11), 110502 (2015)
45. L. Robledo, L. Childress, H. Bernien, B. Hensen, P. F. A. Alkemade, and R. Hanson, High-fidelity projective readout of a solid-state spin quantum register, *Nature* 477(7366), 574 (2011)
46. M. V. G. Dutt, L. Childress, L. Jiang, E. Togan, J. Maze, F. Jelezko, A. S. Zibrov, P. R. Hemmer, and M. D. Lukin, Quantum register based on individual electronic and nuclear spin qubits in diamond, *Science* 316(5829), 1312 (2007)
47. F. Shi, X. Rong, N. Xu, Y. Wang, J. Wu, B. Chong, X. Peng, J. Kniepert, R. S. Schoenfeld, W. Harneit, M. Feng, and J. Du, Room-temperature implementation of the Deutsch—Jozsa algorithm with a single electronic spin in diamond, *Phys. Rev. Lett.* 105(4), 040504 (2010)
48. T. van der Sar, Z. H. Wang, M. S. Blok, H. Bernien, T. H. Taminiau, D. M. Toyli, D. A. Lidar, D. D. Awschalom, R. Hanson, and V. V. Dobrovitski, Decoherence-protected quantum gates for a hybrid solid-state spin register, *Nature* 484(7392), 82 (2012)
49. S. Arroyo-Camejo, A. Lazariev, S. W. Hell, and G. Balasubramanian, Room temperature high-fidelity holonomic single-qubit gate on a solid-state spin, *Nat. Commun.* 5(1), 4870 (2014)
50. C. Zu, W. B. Wang, L. He, W. G. Zhang, C. Y. Dai, F. Wang, and L. M. Duan, Experimental realization of universal geometric quantum gates with solid-state spins, *Nature* 514(7520), 72 (2014)
51. E. Togan, Y. Chu, A. S. Trifonov, L. Jiang, J. Maze, L. Childress, M. V. G. Dutt, A. S. Sørensen, P. R. Hemmer, A. S. Zibrov, and M. D. Lukin, Quantum entanglement between an optical photon and a solid-state spin qubit, *Nature* 466(7307), 730 (2010)
52. H. Kosaka and N. Niikura, Entangled absorption of a single photon with a single spin in diamond, *Phys. Rev. Lett.* 114(5), 053603 (2015)
53. H. Bernien, B. Hensen, W. Pfaff, G. Koolstra, M. S. Blok, L. Robledo, T. H. Taminiau, M. Markham, D. J. Twitchen, L. Childress, and R. Hanson, Heralded entanglement between solid-state qubits separated by three metres, *Nature* 497(7447), 86 (2013)
54. B. C. Ren and F. G. Deng, Hyperentanglement purification and concentration assisted by diamond NV centers inside photonic crystal cavities, *Laser Phys. Lett.* 10(11), 115201 (2013)
55. T. J. Wang and C. Wang, Universal hybrid three-qubit quantum gates assisted by a nitrogen-vacancy center coupled with a whispering-gallery-mode microresonator, *Phys. Rev. A* 90(5), 052310 (2014)
56. C. Wang, Y. Zhang, R. Z. Jiao, and G. S. Jin, Universal quantum controlled phase gate on photonic qubits based on nitrogen vacancy centers and microcavity resonators, *Opt. Express* 21(16), 19252 (2013)
57. F. F. Du, Y. T. Liu, Z. R. Shi, Y. X. Liang, J. Tang, and J. Liu, Efficient hyperentanglement purification for three-photon systems with the fidelity-robust quantum gates and hyperentanglement link, *Opt. Express* 27(19), 27046 (2019)
58. Q. Chen, W. Yang, M. Feng, and J. Du, Entangling separate nitrogen-vacancy centers in a scalable fashion via coupling to microtoroidal resonators, *Phys. Rev. A* 83(5), 054305 (2011)
59. M. O. Scully and M. S. Zubairy, Quantum Optics, Cambridge University Press, 1997
60. C. Y. Hu, W. J. Munro, and J. G. Rarity, Deterministic photon entangler using a charged quantum dot inside a microcavity, *Phys. Rev. B* 78(12), 125318 (2008)
61. J. H. An, M. Feng, and C. H. Oh, Quantum-information processing with a single photon by an input—output process with respect to low-Q cavities, *Phys. Rev. A* 79(3), 032303 (2009)
62. B. C. Pursley, S. G. Carter, M. K. Yakes, A. S. Bracker, and D. Gammon, Picosecond pulse shaping of single photons using quantum dots, *Nat. Commun.* 9(1), 115 (2018)
63. R. Albrecht, A. Bommer, C. Deutsch, J. Reichel, and C. Becher, Coupling of a single nitrogen-vacancy center in

diamond to a fiber-based microcavity, *Phys. Rev. Lett.* 110(24), 243602 (2013)

64. B. J. M. Hausmann, B. Shields, Q. Quan, P. Maletinsky, M. McCutcheon, J. T. Choy, T. M. Babinec, A. Kubanek, A. Yacoby, M. D. Lukin, and M. Lončar, Integrated diamond networks for quantum nanophotonics, *Nano Lett.* 12(3), 1578 (2012)
65. J. Teissier, A. Barfuss, P. Appel, E. Neu, and P. Maletinsky, Strain coupling of a nitrogen-vacancy center spin to a diamond mechanical oscillator, *Phys. Rev. Lett.* 113(2), 020503 (2014)
66. K. M. C. Fu, C. Santori, P. E. Barclay, L. J. Rogers, N. B. Manson, and R. G. Beausoleil, Observation of the dynamic Jahn−Teller effect in the excited states of nitrogen-vacancy centers in diamond, *Phys. Rev. Lett.* 103(25), 256404 (2009)
67. L. C. Bassett, F. J. Heremans, C. G. Yale, B. B. Buckley, and D. D. Awschalom, Electrical tuning of single nitrogen-vacancy center optical transitions enhanced by photoinduced fields, *Phys. Rev. Lett.* 107(26), 266403 (2011)
68. P. Siyushev, H. Pinto, M. Vörös, A. Gali, F. Jelezko, and J. Wrachtrup, Optically controlled switching of the charge state of a single nitrogen-vacancy center in diamond at cryogenic temperatures, *Phys. Rev. Lett.* 110(16), 167402 (2013)